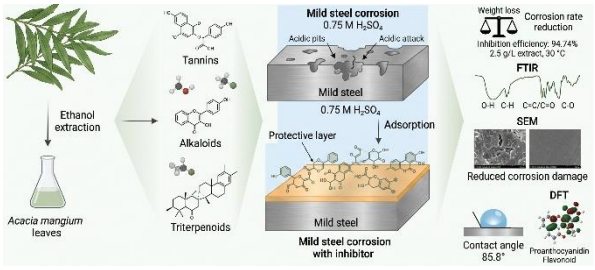
***JKPK (JURNAL KIMIA DAN PENDIDIKAN KIMIA)**, Vol. 11, No. 2, 2026* *pp. 248-266*
Chemistry Education Study Program, Universitas Sebelas Maret *ISSN 2503-4146*
https://jurnal.uns.ac.id/jkpk *ISSN 2503-4154 (online)*

Acacia mangium Leaf Extract as a Green Corrosion Inhibitor for Mild Steel in Sulfuric Acid: Gravimetric Evaluation, Surface Characterization, and Quantum Chemical Descriptor Analysis

Dila Mardiah Permata Sinta[1], Lidia Gusfi Marni[1]*, Diah Riski Gusti[2], Siti Zulaiha[1], Anggela Tria Amanda[1], Emriadi[3], Imelda[3]

[1]Department of Chemistry, Faculty of Science and Technology, UIN Sulthan Thaha Saifuddin Jambi, Jambi, Indonesia.
[2]Department of Chemistry, Faculty of Science and Technology, Universitas Jambi, Jambi, Indonesia.
[3]Department of Chemistry, Faculty of Mathematics and Natural Sciences, Universitas Andalas, Padang, Indonesia

ABSTRACT



Corrosion is the degradation of metallic materials that can compromise their durability, particularly under acidic conditions. This study aimed to evaluate the effectiveness of *Acacia mangium* leaf extract as a green corrosion inhibitor for mild steel in 0.75 M H_2SO_4 solution. The inhibition performance was investigated using weight-loss measurements, adsorption isotherm analysis, and evaluation of thermodynamic parameters. Various extract concentrations (0.5, 1.0, 1.5, 2.0, and 2.5 g/L) were evaluated at different temperatures (30, 40, 50, and 60 °C). Surface characterization using Fourier transform infrared spectroscopy (FTIR), scanning electron microscopy (SEM), and contact angle measurements was performed to elucidate the interaction between the extract compounds and the steel surface. Then the experimental result were confirmed by quantum chemical calculations using at B3LYP/6-311G (d,p). The results demonstrated that the corrosion rate of mild steel decreased progressively with increasing *Acacia mangium* leaf extract concentration. The maximum inhibition efficiency of 94.74% was achieved at 30 °C with an extract concentration of 2.5 g/L. The thermodynamic parameters, including ΔG_{ads} (-16.8825 kJ mol^{-1}), ΔH_{ads} (-45.0793 kJ mol^{-1}), and ΔS_{ads} (-93.0588 J mol^{-1} K^{-1}), indicated that the adsorption process was spontaneous, exothermic, and predominantly governed by a physisorption mechanism. FTIR analysis revealed that functional groups including O–H, C–H, C=C, C=O, and C–O contributed to the adsorption of extract molecules onto the steel surface, while SEM analysis confirmed reduced surface deterioration after inhibitor addition. Furthermore, contact angle measurements demonstrated an increase in surface hydrophobicity, supporting the formation of a protective layer on the mild steel surface. DFT calculations revealed favorable electronic properties of flavonoid and proanthocyanidin for corrosion inhibition.

Keywords: *Acacia mangium leaves; corrosion inhibitor; DFT; mild steel; weight loss*
**Corresponding Author: lidiagusfimarni@uinjambi.ac.id*
How to cite: D. M. P. Sinta, L.G. Marni, D. R. Gusti, S. Zulaiha, A. T. Amanda, E. Emriadi, I. Imelda "Acacia mangium Leaf Extract as a Green Corrosion Inhibitor for Mild Steel in Sulfuric Acid: Gravimetric Evaluation, Surface Characterization, and Quantum Chemical Descriptor Analysis," *Jurnal Kimia dan Pendidikan Kimia (JKPK)*, vol. 11, no. 2, pp. 248–266, 2026. [Online]. Available: https://doi.org/10.20961/jkpk.v11i2.124553
Received: 2026-07-21 *Accepted: 2026-08-25* *Published: 2026-08-31*

INTRODUCTION

Metal is a widely used material in various industries, including construction, metallurgy, petroleum, and aerospace, due to its excellent physical and chemical properties as well as high ductility [1]. However, metals are susceptible to corrosion when exposed to environmental conditions, which can significantly reduce

© 2026 The Authors. This open-access article is distributed under a (CC-BY-SA License)

the service life of metallic equipment [2]. Corrosion is a degradation process involving the deterioration or damage of metal materials through interactions, including ion exchange, between the metal surface and its surrounding environment [3]. Metals tend to react with their surroundings to achieve a more thermodynamically stable state through the formation of oxide or hydroxide compounds [4]. Although corrosion cannot be completely eliminated, its progression can be effectively controlled and reduced [5]. The degradation of metals and alloys negatively affects their mechanical properties and functional performance. Corrosion may lead to infrastructure failure, damage to steel storage tanks, oil leakage, environmental contamination, and even potential loss of human life [6]. Therefore, effective corrosion control strategies are essential, one of which involves the application of corrosion inhibitors [7].

Corrosion inhibitors are chemical substances or compounds employed to reduce or control metal deterioration caused by corrosive environments. The effectiveness of corrosion inhibitors can be evaluated through both experimental and theoretical approaches. Experimental investigations commonly involve techniques such as gravimetric measurements and surface morphology characterization [8]. These methods are applied to assess inhibition performance, investigate corrosion mechanisms, evaluate interactions between inhibitors and metal surfaces, and examine changes in surface morphology after inhibitor exposure [9]. In addition to experimental approaches, computational methods have increasingly been applied to predict corrosion inhibition behavior. Density Functional Theory (DFT) is one of the computational techniques widely utilized in materials science and chemistry, including corrosion research [10]. DFT simulations provide valuable molecular-level information through parameters such as frontier molecular orbital energies and other electronic descriptors, which can be used to explain adsorption behavior and predict the corrosion inhibition capability of compounds [11].

This study investigated the potential application of *Acacia mangium* leaves as a corrosion inhibitor. *Acacia* leaves contain various bioactive compounds that may contribute to corrosion inhibition performance. Tezeghdenti et al. [12] reported that *Acacia cyanophylla* leaf extract exhibited corrosion inhibition properties, attributed to the presence of tannins and flavonoids, with an inhibition efficiency reaching 84%. Similarly, Minagalavar et al. [13] investigated *Acacia melanoxylon* leaves as a corrosion inhibitor and reported an inhibition efficiency of 99.35%. Another study conducted by Jimoh and Usman [14] evaluated *Acacia nilotica* leaves and demonstrated an inhibition efficiency of 87.57%. These findings indicate that various *Acacia* species possess promising potential as natural corrosion inhibitors.

Several *Acacia* species have demonstrated significant corrosion inhibition performance; however, studies investigating *Acacia mangium* leaves as corrosion

inhibitors remain limited. Further investigation is required to evaluate their inhibition capability and elucidate the underlying mechanism. This study aims to analyze the corrosion inhibition ability of *Acacia mangium* leaf extract on steel exposed to sulfuric acid (H_2SO_4) solution and to understand the corresponding inhibition mechanism.

The proposed hypothesis is that bioactive compounds in *Acacia mangium* leaf extract adsorb onto the steel surface and form a protective layer that reduces corrosion. This hypothesis was evaluated through corrosion inhibition testing and surface characterization using weight loss measurements, FTIR, contact angle analysis, SEM, and DFT simulations. The findings provide insight into the inhibition mechanism of *Acacia mangium* extract and its potential as an environmentally friendly corrosion inhibitor.

METHODS

1. Materials and Instruments

The materials used in this study included *Acacia mangium* leaves, technical-grade 96% ethanol, distilled water, concentrated sulfuric acid (H_2SO_4), technical-grade acetone, $FeCl_3$ (Gifala Laboratorium Centre), Mg powder (Sentra Chemicals Indonesia), concentrated hydrochloric acid (HCl), Dragendorff's reagent (Sentra Chemicals Indonesia), Liebermann–Burchard reagent (Sentra Chemicals Indonesia), and mild steel. The equipment used in the study included an analytical balance, a digital USB microscope (Microscope Endoscope 1600X USB Digital), Fourier Transform Infrared (FTIR) spectroscopy (PerkinElmer Spectrum IR Version 10.6.1), Scanning Electron Microscopy (SEM), 100- and 180-grit sandpaper, and other laboratory glassware.

2. *Acacia mangium* Leaf Extraction

Acacia mangium leaves were collected from the UIN STS Jambi Campus. This extraction process refers to the method of Pandey [15] with several modifications. The collected *Acacia mangium* leaves were then dried in a shaded place, then ground using a blender. A total of 550 grams of the simplicia is soaked in 1.75 liters of ethanol for 3 days. After that, they were filtered and the residue is redissolved in 1.25 liters of ethanol for 2 days, then the filtrate was taken. The obtained filtrate was concentrated using a rotary evaporator at 50°C to obtain a viscous crude extract, which was then dried again in a water bath.

3. Phytochemical Testing of *Acacia mangium*

The extract solution for the phytochemical test was prepared by weighing 1 gram of *Acacia mangium* leaf extract and dissolving it in 100 mL of ethanol. The tannin test was performed by adding $FeCl_3$ reagent to the acacia leaf extract. The tannin test shows a positive result with a dark blue or black color change. Flavonoid test was carried out by adding Mg powder and concentrated HCl. A positive flavonoid result is indicated by a yellow or red color change in the solution. The alkaloid test used Dragendroff's reagent added to the acacia leaf extract. A positive

result is indicated by the formation of an orange precipitate. The saponin test was carried out by adding distilled water to the extract solution and then shaking it. A positive result for saponins is obtained if foam forms after being left for 10-15 minutes [16]. The triterpenoid and steroid tests used Lieberman-Buchard reagent. A color change to blue or green indicates the presence of steroids, while a reddish-brown color indicates the presence of terpenoids [17].

4. Preparation of Mild Steel Samples

Mild steel specimens were cut into pieces with dimensions of approximately 2 × 1 cm and drilled to facilitate handling during the corrosion test. The surface of each specimen was mechanically polished using sandpaper to remove surface impurities and obtain a uniform surface condition. The specimens were then rinsed with distilled water, cleaned with acetone, and allowed to dry completely. The initial mass of each specimen was subsequently measured using an analytical balance and recorded as the initial mass (m_1).

5. Weight Loss Measurements

Mild steel was immersed for 3 hours in 50 mL of 0.75 M H_2SO_4 without inhibitor and with inhibitor concentrations of 0.5, 1.0, 1.5, 2.0, and 2.5 g/L. The immersion experiments were conducted at 30, 40, 50, and 60 °C. After immersion, the mild steel was washed with distilled water and acetone and then dried. After drying, the mild steel was weighed and the final mass (m_2) was recorded. The corrosion rate (CR) and inhibition efficiency (IE%) were calculated using the following equations [5], [7]:

$$\mathrm{CR} = \frac{\mathrm{m_1 - m_2}}{\mathrm{A \times t}} \quad (1)$$

$$\%\mathrm{IE} = \left(\frac{\mathrm{Cr_1 - Cr_2}}{\mathrm{Cr_1}}\right) \times 100\% \quad (2)$$

$$\theta = \frac{\mathrm{W}_o - \mathrm{W}_i}{\mathrm{W}_o} \quad (3)$$

where m_1 is the initial weight of steel (g), m_2 is the final weight of steel (g), A is the surface area (cm^2), t is the immersion time of steel (hours), Cr_1 is the corrosion rate of blank, Cr_2 is the corrosion rate of steel with the addition of inhibitor, where W_o represents the corrosion rate in the absence of an inhibitor, while W_i represents the corrosion rate in the presence of an inhibitor.

6. Adsorption Isoterms and Thermodynamics

Adsorption isotherms are an important approach to explaining the interaction mechanism between inhibitor molecules and metal surfaces. The isotherm model that best describes the adsorption of *Acacia mangium* leaf extract inhibitors on mild steel surfaces was analyzed through the relationship between inhibitor concentration (C) and surface coverage (θ). The experimental data were then matched with several adsorption isotherm models, including Langmuir, Freunlich, Temkin, and El-Awady. The linear equations for each isotherm model used in this study are shown in equations (4) – (7) [7]:

$$\frac{\mathrm{C}}{\theta} = \frac{1}{\mathrm{K_{ads}}} + \mathrm{C} \quad (4)$$

$$\log\theta = \log \mathrm{K_{ads}} + \frac{1}{\mathrm{n}}\log\mathrm{C} \quad (5)$$

$$\theta = \frac{-2{,}303\log\mathrm{K_{ads}}}{2\mathrm{a}} - \frac{2{,}303\log\mathrm{C}}{2\mathrm{a}} \quad (6)$$

$$\log\left(\frac{\theta}{1-\theta}\right) = \log K^{i} + y\log C \quad (7)$$

The thermodynamic parameter value of adsorption free energy (ΔG_{ads}) was calculated using equation (8) [18]. The adsorption enthalpy and adsorption entropy were obtained using equation (9) – (10) [19]:

$$\Delta G^{\circ}_{ads} = -RT \ln (55{,}5 \times K_{ads}) \quad (8)$$

$$\ln K_{ads} = constant - \frac{\Delta H^{\circ}}{R}\frac{1}{T} \quad (9)$$

$$\Delta S^{\circ}_{ads} = \frac{\Delta H^{\circ}_{ads} - \Delta G^{\circ}_{ads}}{T} \quad (10)$$

where R and T are the molar gas constant and absolute temperature respectively, and 55.5 is the molar concentration of water in the solution.

7. FTIR, SEM, and Contact Angle Measurement

Test samples were immersed in 0.75 M H_2SO_4 both without an inhibitor and with the addition of 2.5 g/L of inhibitor at room temperature for 3 days. They were then washed with distilled water and acetone, dried and analyzed using SEM. The corrosion products formed were scraped off for FTIR analysis. It should be noted that contact angle measurements were performed on the sample surfaces after 3 hours of immersion.

8. Quantum chemical calculation

This study employed the Density Functional Theory (DFT) method with the B3LYP/6-311G(d,p) basis set and Gaussian 09W software for molecular calculations. The test molecules from *Acacia mangium* leaves, as shown in Table 1, were optimized using the DFT method to obtain the optimal molecule. Then, they were analyzed to determine the best inhibitor molecule using quantum parameters. The output data from the optimization results were E_{HOMO}, E_{LUMO}, E_{Total}, and dipole moment. The values obtained are used to calculate quantum chemical parameters including energy gap (ΔE), ionization potential (I), electron affinity (A), electronegativity (χ), hardness (η), softness (σ), electrophilicity (ω), and electron transfer (ΔN) as follows [20], [21]:

$$I = -E_{HOMO} \quad (10)$$

$$A = -E_{LUMO} \quad (11)$$

$$\Delta E = E_{LUMO} - E_{HOMO} \quad (12)$$

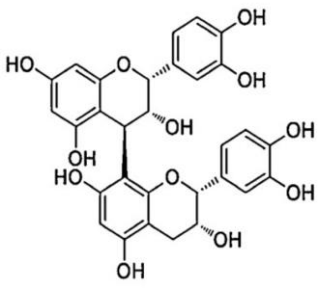
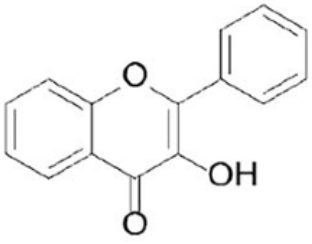
$$\chi = \frac{I+A}{2} \quad (13)$$

$$\eta = \frac{I-A}{2} \quad (14)$$

$$\Delta N = \frac{\varphi_{Fe} - \chi_{inh}}{2(\eta_{Fe} - \eta_{inh})} \quad (15)$$

$$\sigma = \frac{I}{\eta} \quad (16)$$

Table 1. Compounds in *Acacia mangium* leaves

	Proanthocyanidin	Flavonoid	References
Structure			[22]

RESULTS AND DISCUSSION

1. Phytochemical Screening of *Acacia mangium* Leaf Extract

Phytochemical screening is a method that can be used to identify secondary metabolites in natural ingredients. The results of the phytochemical analysis of *Acacia mangium* leaf extract using ethanol are presented in Table 2. The analysis shows that *Acacia mangium* leaf extract contains tannins, flavonoids, alkaloids, and triterpenoids. However, saponins and steroids were not detected in the extract. These secondary metabolites contain heteroatoms such as N and O, which play a crucial role in the adsorption process on metal surfaces to form a protective layer [23]. This indicates that *Acacia mangium* leaf extract has the potential to be used as a natural-based corrosion inhibitor.

Table 2. Results of the phytochemical test of *Acacia mangium* leaf extract

Phytochemical	Reagent	Result
Tanin	$FeCl_3$	+
Flavonoid	Mg + HCl	+
Alkaloid	Dragendroff	+
Saponin	Aquadest	-
Steroid	Liebermann-Burchard	-
Triterpenoid	Liebermann-Burchard	+

2. Weight Loss Analysis

Weight loss analysis was conducted to evaluate the corrosion rate and inhibition efficiency of *Acacia mangium* Leaf Extract on mild steel in a 0.75 M sulfuric acid solution. The data generated includes corrosion rate (g/cm^2.h), inhibition efficiency (%), and surface coverage (θ) presented in Table 3. Measurements were made at various *Acacia mangium* leaf extract concentrations (0.5; 1; 1.5; 2; 2.5 g/L) at temperatures of 30°C, 40°C, 50°C, and 60°C. The results obtained include the corrosion rate, which is presented in Figure 1.

Figure 1 illustrates the downward trend in the corrosion rate as the concentration of *Acacia mangium* leaf extract increases. This reduction indicates that inhibitor molecules adsorb onto the steel surface, forming a protective layer that limits the steel's interaction with the sulfuric acid solution [24]. This phenomenon is attributed to surface coverage (θ) by the Acacia mangium leaf extract molecules, which reduces the active surface area of the steel susceptible to attack by the corrosive solution [21]. Based on weight-loss analysis, the inhibition efficiency values were determined and are presented in Figure 2.

The inhibition efficiency increased with increasing extract concentration, reaching a maximum value of 94.74% at 2.5 g/L and 30°C. As shown in Table 3, efficiency increased from 87.37% to 94.74% with increasing concentration but decreased to 85.32% at higher temperatures. This trend agrees with El-Haddad and Fouda [25], who reported that inhibitor efficiency decreases with increasing temperature. This decrease in adsorption indicates that the desorption of *Acacia mangium* leaf extract molecules from the steel surface increases at higher acidic solution temperatures. This behavior suggests that the *Acacia mangium* leaf extract extract adheres to the steel surface through physical adsorption involving weak bonds.

Table 3. Inhibition efficiency and corrosion rate of steel without and with various extract inhibitors in 0.75 M H_2SO_4 at temperatures of 30 ℃ - 60 ℃.

Temperature	Concentration (g/L)	Corrosion rate ($\times 10^{-2}$ g cm^2 h^{-1})	Inhibition efficiency (%)	Surface coverage (θ)
30 ℃	Blank	1,303	-	-
	0,5	0,165	87,37	0,8737
	1	0,132	89,90	0,8990
	1,5	0,091	93,04	0,9304
	2	0,078	94,02	0,9402
	2,5	0,069	94,74	0,9474
40 ℃	Blank	2,370	-	-
	0,5	0,471	80,13	0,8013
	1	0,375	84,19	0,8419
	1,5	0,270	88,60	0,8860
	2	0,206	91,30	0,9130
	2,5	0,167	92,96	0,9296
50 ℃	Blank	3,868	-	-
	0,5	1,144	70,42	0,7042
	1	0,636	83,55	0,8355
	1,5	0,502	87,02	0,8702
	2	0,431	88,85	0,8885
	2,5	0,410	89,41	0,8941
60℃	Blank	5,377	-	-
	0,5	2,395	55,45	0,5545
	1	1,505	72,01	0,7201
	1,5	1,190	77,87	0,7787
	2	0,990	81,59	0,8159
	2,5	0,789	85,32	0,8532

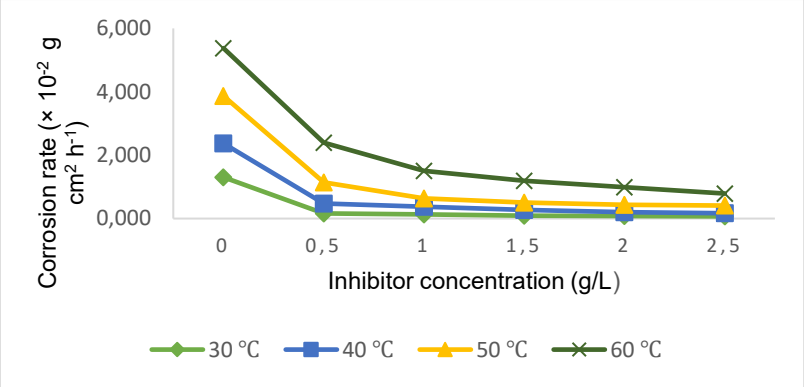


Figure 1. Effect of concentration on the corrosion rate of mild steel in 0.75 M H_2SO_4

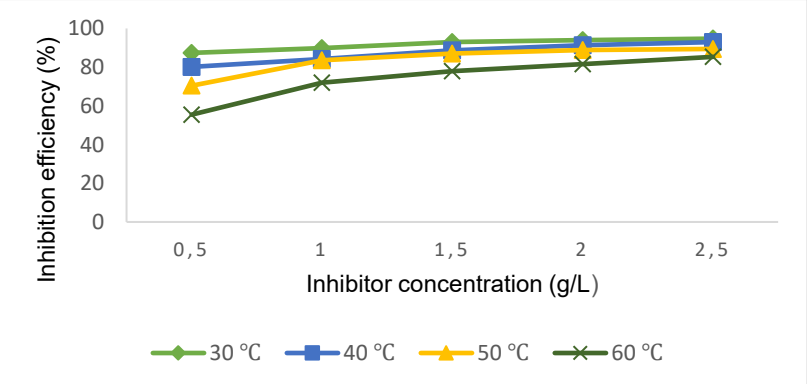


Figure 2. Effect of concentration on corrosion inhibition efficiency on mild steel in 0.75 M H_2SO_4

3. Adsorption Isoterm Analysis and Thermodynamics

Adsorption isotherms describe the relationship between adsorbate and adsorbent molecules at an interface in equilibrium. When a mild steel coupon is immersed in an acidic solution containing an inhibitor, water molecules are immediately adsorbed onto the steel surface and are then gradually replaced by inhibitor molecules. This process causes a decrease in the corrosion rate on the metal surface [15]. The adsorption isotherms tested include the Langmuir, Freundlich, Temkin, and El-Awady isotherms. The linearization results of the Langmuir, Freunlich, Temkin, and El-Awady isotherm models are shown in Figure 3.

The Langmuir isotherm model assumes that adsorption occurs at active sites that can only be occupied by a single inhibitor molecule, thus forming a monolayer on the steel surface [26]. The Freundlich model takes into account surface heterogeneity, multilayer adsorption, and differences in affinity between inhibitor molecules and the metal surface [23]. The Temkin isotherm accounts for interactions between adsorbed species and assumes that the adsorption energy decreases linearly with increasing surface coverage [27]. The El-Awady isotherm can be used to analyze the number of water molecules that can be replaced by one inhibitor molecule on a metal surface. A stronger inhibitor-surface interaction than water causes the adsorption of inhibitor molecules and vice versa [28].

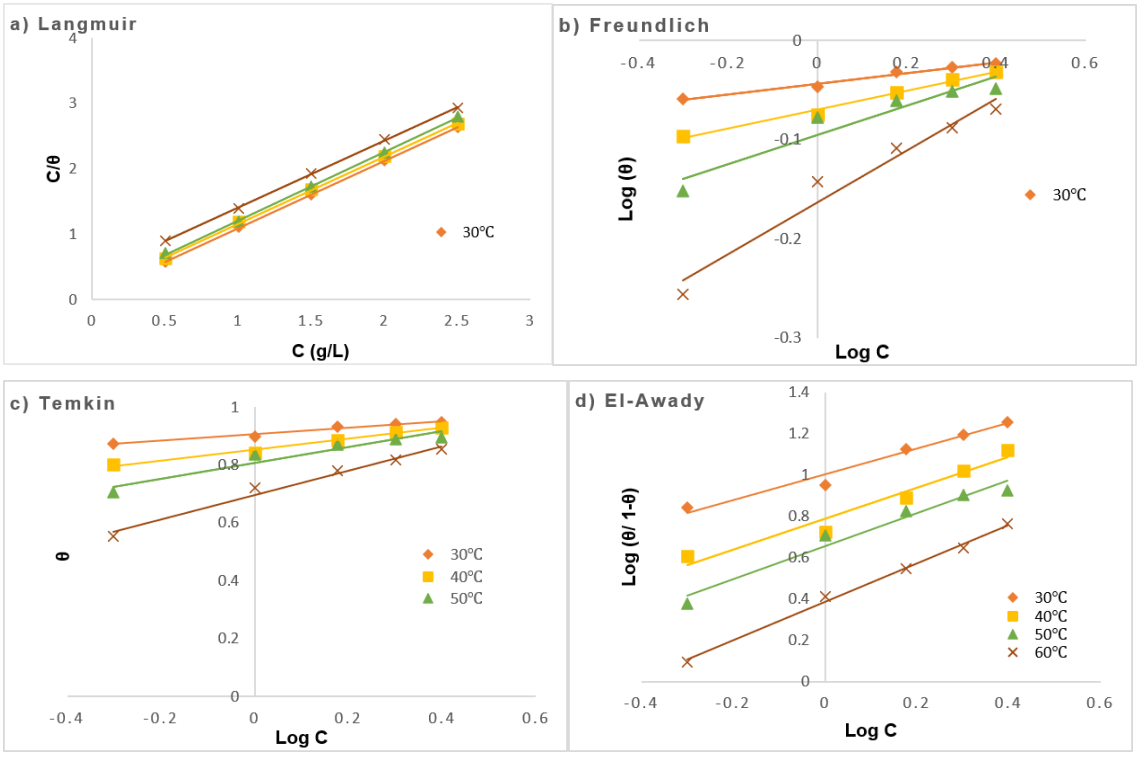


Figure 3. Adsorption isotherms for mild steel in 0.75 M H_2SO_4 medium

Table 4. R^2 values and regression equation

Isoterm	Parameter	R^2	Regression Equations
Langmuir	30 ℃	0.9999	y = 1.0296x + 0.0682
	40 ℃	0.9993	y = 1.0267x + 0.1369
	50 ℃	0.9996	y = 1.0453x + 0.1676
	60 ℃	0.9996	y = 1.0239x + 0.3837
Freunlich	30 ℃	0.9794	y = 0.053x - 0.0434
	40 ℃	0.9885	y = 0.0953x – 0.0699
	50 ℃	0.9081	y = 0.1485x – 0.0952
	60 ℃	0.9632	y = 0.2633x – 0.1631
Temkin	30 ℃	0.9789	y = 0.111x + 0.9054
	40 ℃	0.9855	y = 0.1892x + 0.8526
	50 ℃	0.9216	y = 0.273x + 0.8072
	60 ℃	0.9813	y = 0.4199x + 0.6963
El-Awady	30 ℃	0.9693	y = 0.6202x + 1.0022
	40 ℃	0.9561	y = 0.7444x + 0.7874
	50 ℃	0.9645	y = 0.7979x + 0.6558
	60 ℃	0.9956	y = 0.9308x + 0.3857

Linear regression analysis of the adsorption data provided the R^2 values and regression equations at various adsorption temperatures, as presented in Table 4. The highest correlation coefficient value (approaching 1) at each temperature among all isotherm models tested is the Langmuir isotherm model. Based on the results obtained, the Langmuir isotherm model is the most suitable to describe the adsorption mechanism that occurs between the Acacia mangium leaf extract extract inhibitor and the steel surface. The suitability of this Langmuir model shows that the adsorbed Acacia mangium leaf extract extract molecules form a monolayer on the steel surface. In addition, the Langmuir isoterm model is used to determine the value of thermodynamic parameters including adsorption free energy (ΔG_{ads}), adsorption enthalpy (ΔH_{ads}), and adsorption entropy (ΔS_{ads}) [29].

A negative value of ΔG_ads indicates that the adsorption process of inhibitor molecules onto the mild steel surface occurs spontaneously in the corrosive medium [30]. Based on the magnitude of ΔG_{ads}, adsorption processes with values ≤ -20 kJ mol^{-1} are generally associated with physisorption, whereas values ≥ -40 kJ mol^{-1} are commonly attributed to chemisorption [7]. Physisorption is mainly governed by electrostatic interactions between charged inhibitor species and oppositely charged metal surfaces, while chemisorption involves the formation of coordinate covalent bonds between inhibitor molecules and vacant d-orbitals of metal atoms on the metal surface [27].

Table 5. Thermodynamic parameters

T ℃	K_{ads}	ΔG_{ads} (KJ/mol)	ΔH_{ads} (KJ/mol)	ΔS_{ads} (J/mol)
30	14,6628	-16,8825		-93,0588
40	7,3046	-15,6264	-45,0793	-94,0988
50	5,9666	-15,5823		-91,322
60	2,6062	-13,7716		-94,0173

The thermodynamic parameters obtained at different temperatures are summarized in Table 5. The calculated ΔG_{ads} values ranged from -13.7716 to -16.8825 kJ mol^{-1}, indicating that the adsorption of *Acacia*

mangium leaf extract molecules onto the mild steel surface is spontaneous. These values suggest that the adsorption process is predominantly governed by physical interactions between inhibitor molecules and the metal surface.

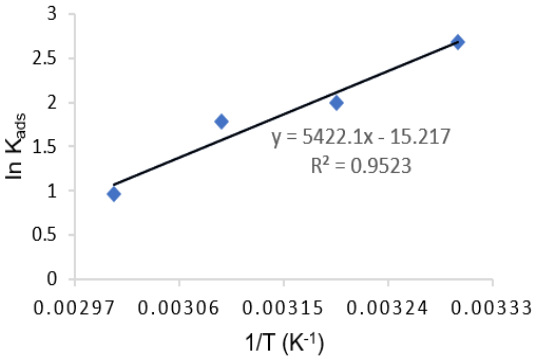


Figure 4. ln Kads vs. 1/T

The enthalpy change of adsorption (ΔH_{ads}) was further evaluated using the van't Hoff relationship between ln K_{ads} and 1/T. As shown in Figure 4, the linear relationship between ln K_{ads} and reciprocal temperature demonstrates the temperature dependence of the adsorption equilibrium. The slope obtained from the regression equation was used to calculate ΔH_{ads} according to the van't Hoff equation. The calculated ΔH_{ads} value was -45.0793 kJ mol^{-1}, indicating that the adsorption process is exothermic, where heat is released during the adsorption of extract molecules onto the mild steel surface [26]. The negative ΔH_{ads} value also suggests that increasing temperature decreases the adsorption tendency, which is consistent with the reduction in inhibition efficiency observed at elevated temperatures.

The entropy change of adsorption (ΔS_{ads}) provides information regarding the change in molecular arrangement and disorder at the inhibitor - metal interface during adsorption [29]. As presented in Table 5, the obtained ΔS_{ads} values were negative at all investigated temperatures, ranging from -91.322 to -94.0988 J mol^{-1} K^{-1}. The negative ΔS_{ads} values indicate a decrease in disorder at the solid–liquid interface, suggesting that inhibitor molecules become more ordered after adsorption onto the mild steel surface [26]. This behavior supports the formation of a stable protective layer consisting of bioactive compounds from *Acacia mangium* leaf extract.

4. Fourier Transform Infrared (FTIR)

Analysis using FTIR was carried out to identify functional groups involved in the formation of protective layers on metal surfaces [31]. FTIR characterization was performed on the *Acacia mangium* leaf extract and steel corrosion products following immersion in the *Acacia mangium* leaf extract inhibitor solution. The spectra obtained from the FTIR characterization are shown in Figure 5.

The FTIR characterization results shown in Figure 5a, it shows the presence of an -OH group at wave number 3322, a C-H group at wave number 2932 and 1447, a C=C/C=O group at wave number 1610, and C-O group at wave numbers 1335 and 1029. Figure 5b shows a shift in the wave number of the -OH group to 3190, the C=C/C=O group shifts at wave number 1636, and the C-O group shifts at wave number 1073.

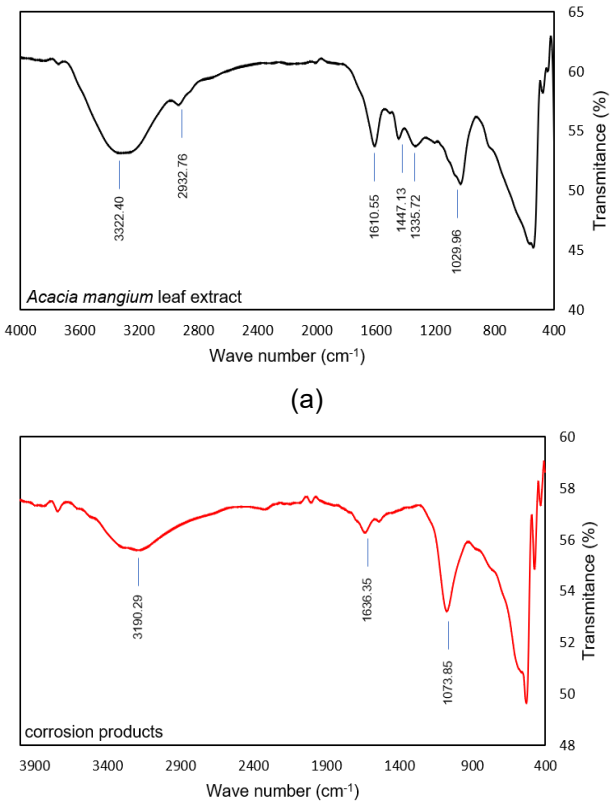


Figure 5. FTIR spectra: (a) *Acacia mangium* leaf extract; (b) mild steel corrosion products in *Acacia mangium* leaf extract inhibitor solution

The comparison of FTIR spectra between *Acacia mangium* leaf extract and the corrosion product formed on the mild steel surface after immersion in the inhibitor solution is presented in Table 6. The FTIR analysis revealed several shifts in the characteristic wavenumbers of functional groups after the adsorption process. The O-H stretching vibration was observed at 3322.40 cm^{-1} in the *Acacia mangium* leaf extract and shifted to 3190.29 cm^{-1} after interaction with the steel surface, corresponding to the hydroxyl functional groups present in the extract. The C-H stretching vibration observed at 2932.76 cm^{-1} was also assigned based on the characteristic range reported in the literature. Furthermore, the absorption bands associated with C=C/C=O functional groups shifted from 1610.55 cm^{-1} to 1636.35 cm^{-1}, indicating possible interactions between these functional groups and the steel surface.

Table 6. Comparison of FTIR spectra

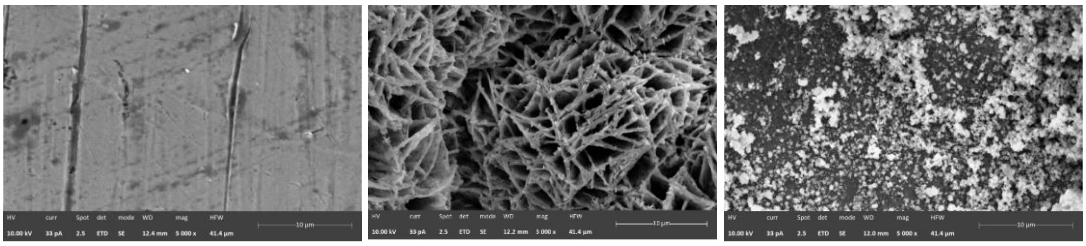
Wave number			Functional groups
Spectrum 5a (cm^1)	Spectrum 5b (cm^1)	Literature [32]	
3322,40	3190,29	3600-3200	O-H
2932,76	-	2960-2860	C-H
1610,55	1636,35	1700-1600	C=C/C=O
1447,13	-	1470-1435	C-H
1335,72	-	1390-1330	C-O
1029,96	1073,85	1150-1040	C-O

The C-H and C-O functional groups also exhibited changes in their characteristic absorption regions. The C-H vibration shifted from 1447.13 cm^{-1}, while the C-O-related absorption bands changed from 1335.72 and 1029.96 cm^{-1} in the extract spectrum to 1073.85 cm^{-1} after adsorption onto the steel surface. These shifts in wavenumber indicate

changes in the chemical environment of the functional groups due to interactions between the bioactive compounds in *Acacia mangium* leaf extract and the mild steel surface. Therefore, the FTIR results support the adsorption of extract constituents onto the steel surface, suggesting that functional groups such as hydroxyl, carbonyl, and C-O groups participate in the formation of a protective adsorption layer during the corrosion inhibition process [33].

5. Scanning Elektron Microscopy (SEM)

Scanning Electron Microscopy (SEM) is an effective tool for analyzing material surface morphology. In this test, SEM helps visualize how inhibitors protect steel from corrosion at the microscopic level [34]. Figure 6a shows the steel surface prior to immersion in 0.75 M H_2SO_4; the surface appears relatively smooth and free of pores, serving as a reference for comparison. Figure 6b displays the steel surface after immersion in 0.75 M H_2SO_4 without an inhibitor, revealing damage in the form of pores, corrosion pits, and a rough surface. In contrast, Figure 6c shows the steel surface after immersion in 0.75 M H_2SO_4 with the addition of *Acacia mangium* leaf extract inhibitor. This figure demonstrates a superior surface condition compared to the uninhibited sample, evidenced by a reduction in the number of pores and corrosion pits, as well as diminished surface damage. SEM observations indicate a change in the steel surface morphology following the addition of the *Acacia mangium* leaf extract inhibitor; this change suggests the formation of a protective layer on the steel surface that helps shield it from corrosion in the corrosive medium [33].



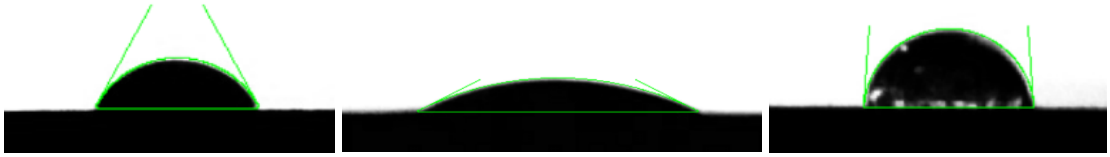
(a) (b) (c)

Figure 6. SEM images of mild steel: a. before immersion in 0.75 M H_2SO_4; b. after immersion in 0.75 M H_2SO_4 without inhibitor; c. after immersion in 0.75 M H_2SO_4 with the addition of *Acacia mangium* leaf extract inhibitor

6. Contact Angle Measurements

The water contact angle on the specimen surface is used as an indicator of surface wettability [35]. Figure 7 illustrates the wetting behavior of water droplets on a steel surface via contact angle measurements. Figure 7a shows the contact angle measurement on the steel surface prior to immersion in a 0.75 M H_2SO_4 solution; the measured water contact angle was 61.2°. Figure 7b displays the contact angle measurement after immersion in 0.75 M H_2SO_4 without an inhibitor. Following immersion in sulfuric acid, the water contact angle decreased to 26.2°, indicating that the surface became more hydrophilic and more easily wetted by water due to the corrosion process. Meanwhile, Figure 7c shows the contact angle measurement after immersion in 0.75 M H_2SO_4 with the addition of an *Acacia mangium* leaf

extract inhibitor. Upon adding the inhibitor, the water contact angle increased to 85.8°. This indicates that the increase in the contact angle value resulted in reduced wettability of the steel surface. This increase can be attributed to the formation of a protective layer resulting from the adsorption of active compound molecules from the extract onto the steel surface which may contribute to a reduction in the corrosion rate [36].



(a) (b) (c)

Figure 7. Contact angle measurements: a. before immersion in 0.75 M H_2SO_4 (contact angle = 61.2°); b. after immersion in 0.75 M H_2SO_4 without inhibitor (contact angle = 26.2°); c. after immersion in 0.75 M H_2SO_4 with the addition of *Acacia mangium* leaf extract inhibitor (contact angle = 85.8°)

7. Quantum Chemical Calculation

Quantum chemical calculations were performed to correlate the experimental findings with the electronic properties of flavonoids and tanin to elucidate their adsorption and inhibition mechanisms. In this study, proanthocyanidins, a class of condensed tannins, were selected as test compounds to facilitate molecular optimization and DFT analysis [21]. The quantum chemical parameters were calculated using DFT at the B3LYP/6-31G(d,p) level, and the optimized molecular structures of the flavonoid and proanthocyanidin compounds are presented in Figure 8.

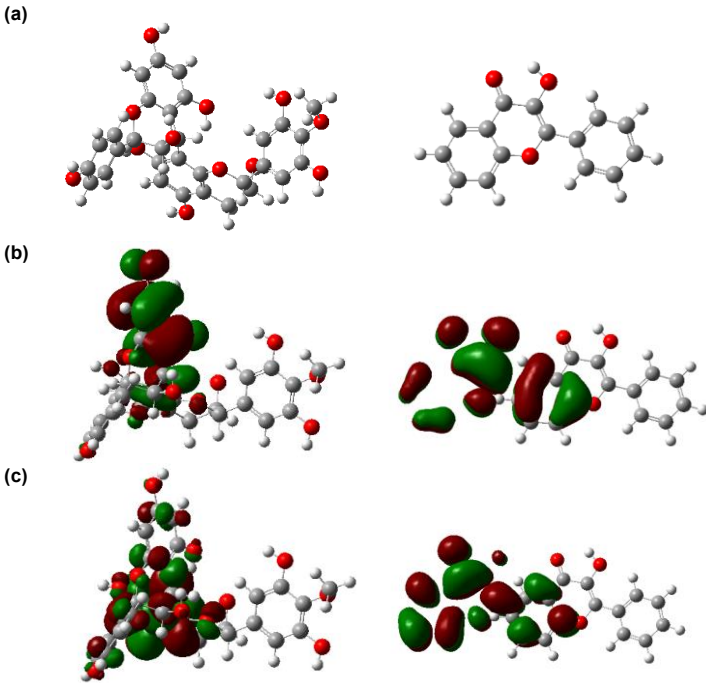


Figure 8. Orbital visualization of proanthocyanidins (left) and flavonoids (right): (a). Molecule optimation, (b). HOMO, (c). LUMO

The optimized structures shown in Figure 8a represent the molecular conformations at their minimum energy state, with proanthocyanidin exhibiting a more complex polyphenolic architecture consisting of multiple condensed aromatic rings, whereas flavonoid displays a comparatively simpler, monocyclic, and planar structure. Figure 8b, the HOMO electron density distribution represented by green (positive phase) and red (negative phase) lobes is predominantly localized around the conjugated aromatic ring systems and phenolic hydroxyl groups of both compounds, indicating that these regions constitute the highest electron density zones and therefore represent potential nucleophilic sites. The HOMO lobes of proanthocyanidin appear more extensive and distributed across several rings simultaneously, consistent with its greater number of aromatic and hydroxyl substituents, whereas the HOMO lobes of flavonoid are relatively more concentrated on a single ring face. Meanwhile, Meanwhile, as shown in Figure 8c, the LUMO distribution appears more dispersed but remains predominantly concentrated over the conjugated aromatic ring systems, although with a different lobe pattern compared with the HOMO.

The quantum chemical parameters of flavonoid and proanthocyanidin are presented in Table 7. These parameters provide insight into the electronic characteristics and potential adsorption behavior of the investigated compounds on the mild steel surface. The HOMO and LUMO energies provide important information regarding the electron-donating and electron-accepting abilities of inhibitor molecules. Flavonoid exhibits a higher HOMO energy (-0.2229 a.u.) than proanthocyanidin (-0.2013 a.u.), indicating a greater tendency to donate electrons to the metal surface. In addition, the lower ionization energy of proanthocyanidin (0.2013 a.u.) compared with flavonoid (0.2286 a.u.) suggests that proanthocyanidin requires less energy for electron donation. The energy gap (ΔE) of flavonoid (0.1417 a.u.) is lower than that of proanthocyanidin (0.2001 a.u.), indicating higher electronic reactivity and a greater ability to interact with the metal surface [13].

Tabel 7. Quantum chemical parameters

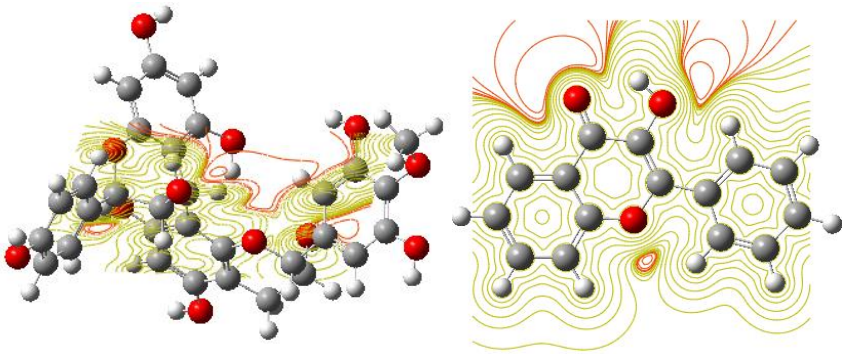
Parameters	Flavonoid	Proanthocyanidin
HOMO energy, E_{HOMO}	-0,2229	-0,2013
Ionization energy, I	0,2286	0,2013
LUMO energy, E_{LUMO}	-0,0812	-0,0012
Electron affinity, A	0,0812	0,0012
Eneregy gap, ΔE	0,1417	0,2001
Dipole moment (Debye)	3,0386	6,5285
E_{Total}, Total Energy (kcal/mol)	-803,4962	-2100,8285
Global electronegativity, χ	0,1549	0,1012
Number of transferred electrons, ΔN	0,2522	0,3451
Global hardness, η	0,0737	0,1000
Global sofness, σ	13,5722	9,9965
$\Delta E_{back\text{-}donation}$	-0,0184	-0,0250

This finding is consistent with the lower global hardness (0.0737 a.u.) and higher softness (13.5722 a.u.) of flavonoid, which suggest greater molecular polarizability and reactivity [37]. Meanwhile, proanthocyanidin exhibits a higher dipole moment (6.5285 D) than flavonoid (3.0386 D), indicating greater

molecular polarity and adsorption capacity [40].

The global electronegativity values of flavonoid and proanthocyanidin are 0.1549 and 0.1012 a.u., respectively. The higher electronegativity of flavonoid indicates a stronger tendency to attract electrons[39]. The fraction of electrons transferred (ΔN) reflects the electron-donating ability of the inhibitor molecules. According to Lukovits [21], when ΔN < 3.6, inhibition efficiency tends to increase with increasing electron-donating ability at the steel interface. As shown in Table 7, all calculated ΔN values are below 3.6, indicating that the investigated compounds have a favorable tendency to donate electrons to the metal surface. The negative $\Delta E_{back\text{-}donation}$ values obtained for flavonoid (-0.0184 a.u.) and proanthocyanidin (-0.0250 a.u.) indicate that electron back-donation is energetically favorable. This interaction can contribute to the stabilization of the inhibitor and metal through a synergistic donor acceptor mechanism [38]. The DFT results indicate that both flavonoid and proanthocyanidin exhibit favorable electronic properties that support their potential as corrosion inhibitors. Flavonoid is characterized by higher electronic reactivity and electronegativity whereas proanthocyanidin exhibits greater polarity and electron-transfer tendency, suggesting that both compounds can interact effectively with the mild steel surface.

Figure 9 shows a contour representation of the distribution of Electrostatic potentials of proanthoanyanidin and flavonoids. Electrostatic potentials maps are used to visualize the distribution of electrons, thereby allowing the identification of the center of the area of electron concentration in each compound. The interaction sites surrounded by dark red contours contribute to the formation of interaction bonds between the metal surface and the inhibitor [41]. The dark red color on the map represents the negative potential contour, while the light green color is distributed in the positive potential region [42]. Based on these characteristics, the negative potential area in Figure 9 appears to specifically surround the oxygen atoms of proanthocyanidins and flavonoids. This indicates that these areas are active centers that facilitate adsorption on metal surfaces



(a) (b)

Figure 9. The contour representation of electrostatic potential (a) proanthoanyanidins and (b) flavonoids

CONCLUSION

The research results demonstrate that Acacia mangium leaf extract demonstrated a corrosion inhibition efficiency of 94.74% on mild steel in 0.75 M H_2SO_4 solution at a concentration of 2.5 g/L and a temperature of 30°C. The adsorption of Acacia mangium leaf extract onto the mild steel surface in 0.75 M H2SO4 solution followed the Langmuir isotherm model, and thermodynamic parameters indicated that the adsorption process was spontaneous and exothermic, tending to follow a physisorption mechanism. FTIR analysis confirmed the involvement of O-H, C-H, C=C, C=O, and C-O functional groups in the adsorption of extract compounds onto the steel surface. SEM characterization revealed a significant reduction in surface damage, while contact angle measurements showed an increase in the contact angle of the mild steel surface. Overall, quantum chemical calculations indicated that flavonoids and proanthocyanidins possess favorable electronic characteristics that facilitate their adsorption onto the mild steel surface, supporting their potential as corrosion inhibitors and the experimental findings.

Author Contributions: D. M. P. Sinta contributed to the conceptualization, methodology, experimental investigation, data collection, data analysis, interpretation of results, and manuscript preparation. L. G. Marni contributed to research supervision, validation, data interpretation, and critical revision of the manuscript. D. R. Gusti contributed to the experimental design, corrosion analysis, discussion of results, and manuscript review. S. Zulaiha and A. T. Amanda contributed to laboratory experiments, material preparation, and data collection. E. Emriadi and I. Imelda contributed to scientific discussion, validation, and manuscript improvement. All authors have read and approved the final version of the manuscript.

Conflict of Interest: The authors declare that they have no known competing financial interests or personal relationships that could have influenced the work reported in this manuscript.

Declaration of Generative AI and AI-Assisted Technologies: Generative artificial intelligence (AI) tools were used during the preparation of this manuscript solely to assist in the development of the graphical abstract and to improve the English language through proofreading and grammatical correction. The authors reviewed and edited all AI-assisted outputs and take full responsibility for the final content of the manuscript.

REFERENCES

[1] Q. Wang *et al.*, “Application of Biomass Corrosion Inhibitors in Metal Corrosion Control: A Review,” Mar. 01, 2023, *MDPI*. doi: 10.3390/molecules28062832.

[2] Q. Shi, S. Deng, D. Xu, D. Shao, G. Du, and X. Li, “Rapeseed cake meal extract as an efficient plant-based inhibitor for the corrosion of steel in Cl2CHCOOH: Experiments and molecular modeling calculations,” *Ind. Crops Prod.*, vol. 225,

Mar. 2025, doi: 10.1016/j.indcrop.2025.120540.

[3] A. A. P. Amaro, A. E. Ares, and C. M. Méndez, "Evaluation of Yerba Mate Extract as a Green Inhibitor for Aluminum Corrosion in 0.5 M HCl," *Coatings*, vol. 16, no. 7, p. 795, Jul. 2026, doi: 10.3390/coatings16070795.

[4] H. M. Hassan, "Prevention of Corrosion in the Stainless Steel Metallic Using the Extract of Some Aquatic Plants," *Chemical Methodologies*, vol. 8, no. 6, pp. 462–477, Jun. 2024, doi: 10.48309/chemm.2024.460575.1800.

[5] D. R. Gusti, A. P. Gunawan, D. Muhammad, and I. Lestari, "A Mixture of Acacia Bark Extract (Acacia mangium Willd) and Potassium Iodide as a Corrosion Inhibitor in Sulfuric Acid Solution," *al-Kimiya*, vol. 10, no. 2, pp. 64–73, Dec. 2023, doi: 10.15575/ak.v10i2.26187.

[6] S. Feliu and F. García-Galvan, "Corrosion and Protection of Metallic Materials," Apr. 01, 2025, *Multidisciplinary Digital Publishing Institute (MDPI)*. doi: 10.3390/met15040346.

[7] C. P. Mungwari, B. A. Obadele, and C. K. King'ondu, "Synergistic corrosion inhibition of 304 stainless steel in 1 M HCl by methanolic Acacia mearnsii bark extract and KI: Thermodynamic, kinetic, and thermal analysis," *Chemical Thermodynamics and Thermal Analysis*, vol. 20, Oct. 2025, doi: 10.1016/j.ctta.2025.100233.

[8] M. B. Pial and M. A. Islam, "The effectiveness of natural corrosion inhibitors in corrosive media," May 01, 2025, *Elsevier B.V.* doi: 10.1016/j.rsurfi.2025.100516.

[9] A. A. Al-Amiery, W. N. R. W. Isahak, and W. K. Al-Azzawi, "Corrosion Inhibitors: Natural and Synthetic Organic Inhibitors," Apr. 01, 2023, *MDPI*. doi: 10.3390/lubricants11040174.

[10] A. I. Ikeuba *et al.*, "Review of computational methods used in the evaluation corrosion inhibition of metallic materials," Dec. 01, 2024, *Discover*. doi: 10.1007/s43938-024-00065-6.

[11] C. Verma, E. E. Ebenso, M. A. Quraishi, and C. M. Hussain, "Recent developments in sustainable corrosion inhibitors: Design, performance and industrial scale applications," Jun. 21, 2021, *Royal Society of Chemistry*. doi: 10.1039/d0ma00681e.

[12] M. Tezeghdenti, N. Etteyeb, L. Dhouibi, O. Kanoun, and A. Al-Hamri, "Natural products as a source of environmentally friendly corrosion inhibitors of mild steel in dilute sulphuric acid: Experimental and computational studies," *Protection of Metals and Physical Chemistry of Surfaces*, vol. 53, no. 4, pp. 753–764, Jul. 2017, doi: 10.1134/S2070205117040219.

[13] R. L. Minagalavar, S. K. Rajappa, M. R. Rathod, and A. M. Sajjan, "Ferrous metal corrosion studies in presence of eco-friendly acacia melanoxylon leaves extract in 1M HCl condition," *Inorg. Chem. Commun.*, vol. 160, Feb. 2024, doi: 10.1016/j.inoche.2023.111900.

[14] I. Jimoh and B. Usman, "Corrosion Inhibition Potential of Ethanol Extract of Acacia nilotica Leaves on Mild Steel in an Acidic Medium," *Portugaliae Electrochimica Acta*, vol. 39, no. 2, pp. 105–133, 2021, doi: 10.4152/pea.202102105.

[15] B. Pandey, D. Pandey, N. P. Pant, D. P. Bhattarai, M. Dhakal, and H. B. Oli, "Methanol extract of Murraya koenigii stem as green inhibitor for mild steel corrosion in 1 M HCl solution," *Results in Surfaces and Interfaces*, vol. 16, Aug. 2024, doi: 10.1016/j.rsurfi.2024.100245.

[16] R. Rahmawati *et al.*, "Identification of Antioxidant Compounds using the DPPH Radical Scavenging Method from Ethanol and Methanol Extracts of the Leaves and Fruits of the Renggak Plant (Ammomum dealbatum R.)," *ALCHEMY Jurnal Penelitian Kimia*, vol. 22, no. 1, p. 217, Mar. 2026, doi: 10.20961/alchemy.22.1.108082.217-227.

[17] Y. T. Situmorang, H. Halimatussakdiah, U. Amna, and V. Mardina, "Phytochemical Examination, GC-MS Analysis, and Antibacterial Activity of Methanol Extract of Dadap Leaves (Erythrina variegata L.) Against

Staphylococcus aureus and Escherichia coli Bacteria using Disc Diffusion Method," *ALCHEMY Jurnal Penelitian Kimia*, vol. 22, no. 1, p. 264, Mar. 2026, doi: 10.20961/alchemy.22.1.99255.264-273.

[18] S. A. Hussein and A. A. Khadom, "Okra leaves extract as green corrosion inhibitor for steel in sulfuric acid: Gravimetric, electrochemical, and surface morphological investigations," *Results Chem.*, vol. 8, Jun. 2024, doi: 10.1016/j.rechem.2024.101566.

[19] A. A. Naser, "Schiff Base-Decorated Graphene Oxide as Corrosion Inhibitor for Carbon Steel Type C1025 in Acidic Solution," *Indonesian Journal of Chemistry*, vol. 25, no. 5, pp. 1526–1539, Oct. 2025, doi: 10.22146/ijc.105964.

[20] T. C. Leboho, K. Selowa, R. K. Mothapo, K. Bokgobelo, T. Pesha, and B. P. Moloto, "Sulfamezarine derivatives as potential corrosion inhibitors for zinc metal in 1 M sulfuric acid solution: Synthesis, experimental, and DFT studies," *Next Research*, vol. 2, no. 3, p. 100702, Sep. 2025, doi: 10.1016/j.nexres.2025.100702.

[21] U. Mamudu, M. S. Alnarabiji, and R. C. Lim, "Adsorption isotherm and molecular modeling of phytoconstituents from Dillenia suffruticosa leaves for corrosion inhibition of mild steel in 1.0 M hydrochloric acid solution," *Results in Surfaces and Interfaces*, vol. 13, Oct. 2023, doi: 10.1016/j.rsurfi.2023.100145.

[22] T. S. Wahyuni, N. S. Sukma, A. A. Permanasari, C. Aoki-Utsubo, A. Widyawaruyanti, and A. F. Hafid, "Acacia mangium: A promising plant for isolating anti-hepatitis C virus agents," *F1000Res.*, vol. 11, p. 1452, Dec. 2023, doi: 10.12688/f1000research.124947.1.

[23] R. E. C. Amon, J. M. C. Quijano, M. C. F. C. Insoy, P. L. T. Nani, and C. F. Y. Lobarbio, "Assessment of Piper siriboa L. (Buyo) leaf extract as a green corrosion inhibitor for carbon steel in hydrochloric acid," *Kuwait Journal of Science*, vol. 53, no. 3, Jul. 2026, doi: 10.1016/j.kjs.2026.100615.

[24] A. Al-Amiery, N. A. Betti, and L. M. Shaker, "Exploring the effectiveness of 3-chloro-4-morpholin-4-yl-1,2,5-thiadiazole as an eco-friendly corrosion inhibitor for mild steel in HCl solution: Experimental and DFT analysis," *Results in Engineering*, vol. 24, Dec. 2024, doi: 10.1016/j.rineng.2024.103014.

[25] M. N. EL-Haddad and A. S. Fouda, "Investigating Xanthium spinosum extract as an eco-friendly corrosion inhibitor for Aluminium in acidic environments: A green approach to metal protection," *Results Chem.*, vol. 14, Mar. 2025, doi: 10.1016/j.rechem.2025.102136.

[26] K. U. Ilyas, E. Budiyati, N. Hidayati, and T. Widayatno, "Thermodynamic Study of Chitosan as a Corrosion Inhibitor for Carbon Steel in Chloride Solutions (NaCl and HCl) at Various Temperatures and Concentrations," *Jurnal Kimia Sains dan Aplikasi*, vol. 27, no. 12, pp. 569–579, Dec. 2024, doi: 10.14710/jksa.27.12.569-579.

[27] A. Al-Amiery and L. M. Shaker, "Green and hybrid corrosion inhibitors from adsorption mechanisms to deployable performance," *Discover Electrochemistry*, vol. 3, no. 1, p. 54, Jun. 2026, doi: 10.1007/s44373-026-00141-2.

[28] A. A. Adamu, O. R. A. Iyun, and J. D. Habila, "Adsorption and thermodynamic studies of the corrosion Inhibition effect of Desmodium adscendens (Swartz) extract on carbon steel in 2 M HCl," *BMC Chem.*, vol. 19, no. 1, Dec. 2025, doi: 10.1186/s13065-025-01541-y.

[29] D. R. Gusti *et al.*, "Eco-friendly corrosion inhibitors (combination of Macaranga gigantea sap extract and maltodextrin) on mild steel in sulfuric acid media," *Results in Surfaces and Interfaces*, vol. 23, May 2026, doi: 10.1016/j.rsurfi.2026.100762.

[30] M. Pourmohseni, A. Rashidi, and M. Karimkhani, "Preparation of corrosion inhibitor from natural plant for mild stil immersed in an acidic environmental: experimental and theoretical study," *Sci. Rep.*, vol. 14, no. 1, Dec. 2024, doi: 10.1038/s41598-024-58637-z.

[31] O. A. Elgyar, M. E. Yassen, A. M. Ouf, A. El-Hossiany, and A. E. A. S. Fouda,

"Insight into the anti-corrosion performance of capparis spinoza extract as a green corrosion inhibitor for carbon steel in hydrochloric acid environment," *Sci. Rep.*, vol. 15, no. 1, Dec. 2025, doi: 10.1038/s41598-025-30968-5.

[32] J. B. Johnson, K. B. Walsh, M. Naiker, and K. Ameer, "The Use of Infrared Spectroscopy for the Quantification of Bioactive Compounds in Food: A Review," Apr. 01, 2023, *MDPI*. doi: 10.3390/molecules28073215.

[33] Y. Stiadi, Emriadi, Rahmayeni, S. Anasha, and T. P. Wendari, "Anticorrosive effectiveness of mild steel by dragon scale fern (Drymoglossum piloselloides L.) leaf extract in hydrochloric acid medium: A combined experimental and computational approach," *International Journal of Corrosion and Scale Inhibition*, vol. 14, no. 2, pp. 566–588, 2025, doi: 10.17675/2305-6894-2025-14-2-8.

[34] E. K. Alenezy, M. A. Abbas, H. R. Madian, M. Ezzeldien, Y. Sabri, and E. S. Gad, "An investigation into the impact of polyethylene glycol on guava leaf extract as a green corrosion inhibitor for mild steel in sulfuric acid," *Journal of Engineering Research (Kuwait)*, Jun. 2026, doi: 10.1016/j.jer.2026.02.012.

[35] Y. Meng, S. Li, and Z. Zhang, "Inhibition performance of uniconazole on steel corrosion in simulated concrete pore solution: An eco-friendly way for steel protection," *Heliyon*, vol. 10, no. 3, Feb. 2024, doi: 10.1016/j.heliyon.2024.e24688.

[36] R. Rohil, Y. Stiadi, and E. Emriadi, "Cinnamon (Cinnamomum burmanni Nees and T. Nees) leaves extract as green corrosion inhibitor for mild steel in HCl solution," *International Journal of Corrosion and Scale Inhibition*, vol. 14, no. 4, pp. 1798–1812, 2025, doi: 10.17675/2305-6894-2025-14-4-4.

[37] O. S. Al-Qurashi and N. Wazzan, "Molecular and periodic DFT calculations of the corrosion protection of Fe(1 1 0) by individual components of Aerva lanata flower as a green corrosion inhibitor," *Journal of Saudi Chemical Society*, vol. 26, no. 6, Nov. 2022, doi: 10.1016/j.jscs.2022.101566.

[38] Naveenkumar C., Dileep R., and Ranganatha S., "Design and development of thiadiazole derived Schiff base as efficient corrosion inhibitor for steel materials: Experimental and quantum analysis," *Next Materials*, vol. 12, p. 102200, Jul. 2026, doi: 10.1016/j.nxmate.2026.102200.

[39] L. Qiu, X. Li, B. Tan, Y. Xie, and S. Deng, "Agricultural waste of tobacco stem extract as a novel and efficient inhibitor for the corrosion of steel in HCl solution," *Ind. Crops Prod.*, vol. 224, Feb. 2025, doi: 10.1016/j.indcrop.2024.120367.

[40] A. S. Al-Gorair *et al.*, "Assessments of licorice root extract as an environmentally benign corrosion inhibitor for aluminum in HCl solutions," *International Journal of Electrochemical Science* , vol. 21, no. 5, May 2026, doi: 10.1016/j.ijoes.2026.101343.

[41] H. Bourzi *et al.*, "Furfural analogs as sustainable corrosion inhibitors-predictive efficiency using DFT and monte carlo simulations on the Cu(111), Fe(110), Al(111) and Sn(111) surfaces in acid media," *Sustainability (Switzerland)*, vol. 12, no. 8, Apr. 2020, doi: 10.3390/SU12083304.

[42] S. Ksama *et al.*, "Detailed experimental and computation/molecular simulation of 1,5-benzodiazepin derivative as corrosion inhibitor for E24 steel in 1 M HCl environment," *International Journal of Corrosion and Scale Inhibition*, vol. 13, no. 4, pp. 2054–2086, 2024, doi: 10.17675/2305-6894-2024-13-4-9.